Module Dynamics of the GnRH Signal Transduction Network

DAVID C. KRAKAUER*†, KAREN M. PAGE‡ AND STUART SEALFON§

†*Santa Fe Institute, Santa Fe, NM* 87501, *U.S.A*, ‡*Bioinformatics Unit, Department of Computer Science, UCL, Gower St, London WC1E 6BT, U.K. and* §*Departments of Neurology, Neurobiology and Pharmacology, Mount Sinai School of Medicine, New York, NY* 10029, *U.S.A.*

We analyse computational modules of a frequency decoding signal transduction network. The gonadotropin releasing hormone (GnRH) signal transduction network mediates the biosynthesis and release of the gonadotropins, luteinizing hormone (LH) and follicle stimulating hormone (FSH). The pulsatile pattern of GnRH production by the hypothalamus has a critical influence on the release and synthesis of gonadotropins in the pituitary. In humans, slower pulses lead to the expression of the β-subunit of the LH protein and cause anovulation and amenorrhea. Higher frequency pulses lead to expression of the α subunit and a hypogonadal state. The frequency sensitivity is a consequence of the structure of the GnRH signal transduction network. We analyse individual components of this network, organized into three network architectures, and describe the frequency-decoding capabilities of each of these modules. We find that these modules are comparable to simple circuit elements, some of which integrate and others which perform as frequency sensitive filters. We propose that the cell computes by exploiting variation in the time scales of protein activation (phosphorylation) and gene expression.

© 2002 Elsevier Science Ltd. All rights reserved.

Structure of the GnRH Signal Transduction Network

The gonadotropic releasing hormone (GnRH) system has been called the prototype of periodic hormone signaling (Li & Goldbetter, 1989; Goldbeter *et al.*, 1990). The frequency of secretion is different in various mammalian species and varies during the reproductive cycle. In humans females, for example, GnRH pulses are least frequent during the mid- and late-luteal stages, where they occur on average every 6 hr. Maximal GnRH secretion frequency, which occurs during the follicular and early luteal

stages, has a period of approximately 90 min. The pulse durations are on the order of 10 min. Disruption of the normal pattern of GnRH secretion is associated with reproductive disorders in both males and females (Crowley *et al.*, 1985). The frequency of secretion is higher in rodents, achieving a maximal period of approximately 30 min.

GnRH acts on the pituitary gonadotrope to regulate the biosynthesis and secretion of the gonadotropins luteinizing hormone (LH) and follicle stimulating hormone (FSH). The subject of our investigation is the regulation of gonadotropin biosynthesis. The gonadotropin hormones consist of two subunits, a common α-subunit and a distinct β-subunit (LHβ or FSHβ). The GnRH pulse frequency changes

*Corresponding author. Santa Fe Institute, Hyde Park Road, Santa Fe, NM 87501, U.S.A.

E-mail address: krakauer@santafe.edu (D. C. Krakauer).

under various physiological conditions, and varying frequencies have been shown to regulate differentially the expression of the common α-subunit, LHβ, and FSHβ subunit genes *in vivo* (Dalkin *et al.*, 1989; Haisenleder *et al.*, 1991) and *in vitro* (Weiss *et al.*, 1990; Shupnik, 1990; Kaiser *et al.*, 1997; Turgeon *et al.*, 1996; Weck *et al.*, 2000). In general, in the rodent gonadotrope, the α-subunit responds to constant exposure or high-pulse frequency (period at around 10 min), whereas the LHβ-subunit promoter responds best to lower frequency pulses (period at around 30–60 min) and FSHβ to even lower frequencies.

GnRH achieves its effects at the pituitary gonadotropes by interaction with a heptahelical G-protein coupled receptor (Sealfon *et al.*, 1997). Activation of the GnRH receptor stimulates a variety of intracellular signaling pathways, including phospholipase C, phospholipase D, phospholipase A2, calcium, protein kinase C and mitogen-activated protein kinases (MAPK) (Naor *et al.*, 1998, 2000; Cheng & Leung 2000). The activation of the MAPK cascades culminates in the induction of specific genes.

Activation of MAPK signaling has been implicated in the induction of both the α- and LHβ-subunit. Most studies indicate that activation of the MAPK ERK is required for GnRH-stimulated α-subunit induction, most likely by phosphorylation and thereby activating an Ets family transcription factor (Roberson *et al.*, 1995; Weck *et al.*, 1998, 2000; Maurer *et al.*, 1999). Ets-family transcriptions factors are directly activated by MAPK phosphorylation, leading to gene transcription (Yordy & Muise-Helmericks, 2000).

Whereas the common α subunit appears to be inducible by phosphorylation of a transcription factor, the LHβ promoter requires the new synthesis of the transcription factor egr1 for activation. GnRH also induces the expression of several other early gene transcription factors (Wurmbach *et al.*, 2001). Several studies suggest that the presence of other transcription factors in addition to egr1 may be required for LHβ gene activation by GnRH (Weck *et al.*, 2000; Tremblay & Drovin 1999; Kaiser *et al.*, 1998; Sevetson *et al.*, 2000). One recent study implicates activation of c-Jun NH2-terminal kinase (JNK) and c-Jun in LHβ-induction (Yokoi *et al.*, 2000).
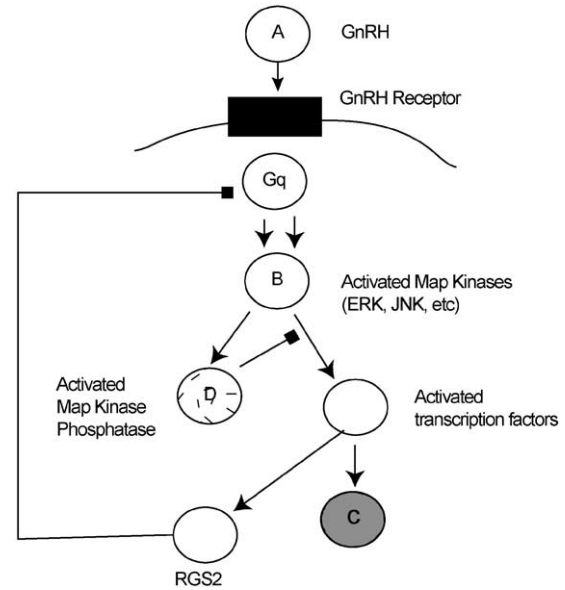

FIG. 1. Schematic illustration of the principal signaling events involved in gonadotropin synthesis. (A) represents the circulating GnRH released periodically from the hypothalamus. GnRH binds to the GnRH receptor on the surface of gonadotrope cells of the pituitary. This leads to the fast activation through phosphorylation of map kinases (B). These can then activate map kinase phosphatases (D) which feed back to dephosphorylate map kinases. They (B) are also able to activate transcription factors leading to the slow synthesis of further transcription factors such as egr1 and RGS2 (C). These can feed back to inhibit the activation of MAPKs, or trigger downstream events culminating in the production of FSH and LH. The precise nature of the connections between components and possible signal intermediates remain to be determined. Lines ending with arrow heads are excitatory, whereas lines ending with blocks are inhibitory.

Based on the experimental literature, several modular structures can be suggested to represent the connectivity between the terminal MAPK signaling cascade and the gonadotropin genes. In essence, the induction of the α-subunit requires activation of a terminal MAPK and phosphorylation of an ets-family transcription factor. The induction of the LHβ-subunit, requires synthesis of one or more early gene transcription factors. The newly synthesized transcription factors, possibly in concert with phosphorylation of other transcription factors, induce, in concert, the LHβ gene (see Fig. 1).

DECONSTRUCTING THE GNRH NETWORK

The secretion of pre-synthesized gonadotropins has been the focus of important earlier

theoretical work (Goldbeter *et al.*, 1988; Li & Goldbetter 1989, 1992; Blum *et al.*, 2000). In these models, receptor desensitization plays an essential role in modulating secretion. Increasing the frequency of receptor stimulation leads, in the limiting case of very high frequencies, to a response equivalent to that under constant stimulation (Segel *et al.*, 1986). At low frequencies, receptor-resensitization allows for increased responsiveness and higher rates of secretion. There are three important properties of these models that should be stressed: (1) the control exerted over the system by the receptor, (2) the interdependence of signal duration and signal frequency, and (3) the absence of biosynthetic pathways, specifically, the expression of genes regulating the production of gonadotropins. Our investigations differ from this earlier work on all three points. Most importantly, experimental studies over the past decade suggest that the GnRH receptor shows minimal desensitization (see Sealfon *et al.*, 1997). A new intra-cellular theory is required for the extraction of frequency-encoded information.

In this study, we explore the capacity of three models representing selective components of the GnRH signaling network, to contribute to the frequency dependence of the gene responses. We adopt this approach as the precise connectivity of the complete GnRH network has yet to be elucidated, whereas qualitative features of components of the network, have been determined (see above). Our precise objective is to determine how different properties (pulse amplitude, pulse duration, pulse frequency) of the input signal might be represented by different components of the network. We follow Marr's (1982) approach to the visual system in which we determine the computations and algorithms executed by increasingly inclusive subsets of the complete network. The first model is a feed-forward, serial network and neglects feedback [Fig. 2(1)]. The second model is a feed-forward, parallel network [Fig. 2(2)]. The third model is a recurrent, parallel network including negative feedback [Fig. 2(3)]. The models are of varying complexity, as measured by the inclusion or exclusion of feedback, and the inclusion or exclusion of parallel pathways.
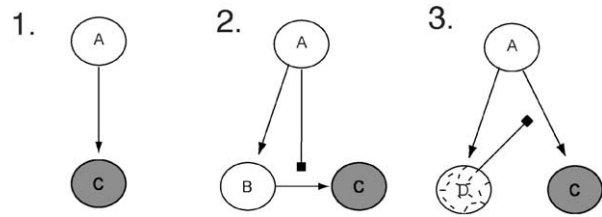

FIG. 2. Three putative modules inspired by the GnRH network. Each of the three modules is derived by removing two to three components and their connections from the full schematic in Fig. 1. Each module is shown in this paper to extract different features from the input signal (periodic presentation of GnRH at the GnRHR). Lines ending with arrow heads are excitatory, whereas lines ending with blocks are inhibitory.

Each of these models produces a distinct pattern of activation, and each varies in the degree to which it can independently parse amplitude-encoded information, from pulse duration and frequency-encoded information. We do not offer formal models for how module outputs are translated into differential gene activation. Empirically, the relationship of transcription factor concentration or phosphorylation, to gonadotrope gene expression, remains unquantified and the subject of intensive research. We restrict ourselves to exploring the response properties of proximal components of the network.

Model 1: Feed-forward Serial Network

Upon stimulation of the GnRHR with pulsatile GnRH, there is a rapid activation of the mitogen-activated kinases, MAPK. Through the phosphorylation of transcription factors these lead to the eventual activation of the egr1 gene and the production of egr1 and label GnRH species A and egr1 species C [Fig. 2(1)]. We denote the concentrations of A and C by a and c, respectively. C is assumed to decay naturally at a rate δ. The dynamics of c are given by

$$\dot{c} = h(a(t - \sigma)) - \delta c, \qquad (1)$$

where t is time, h is some Hill-like function, reflecting the fact that A does not directly induce C, but is activated via an intermediate cascade. σ is a delay introduced by protein translation. We now suppose that A is a cycling chemical, that is $a(t + \tau) = a(t)$, for some time period τ
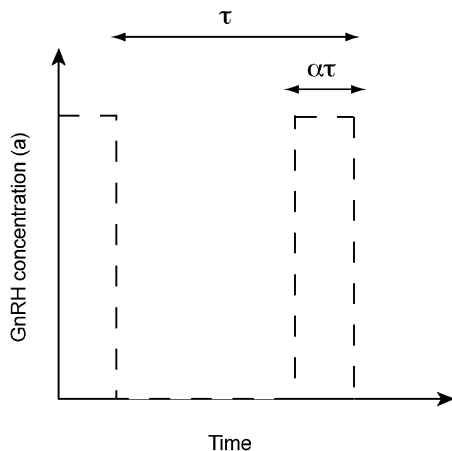
FIG. 3. The pulsatile presentation of GnRH at the GnRH receptor. GnRH pulses with an inter-pulse period of τ. The pulse duration is $\alpha\tau$.

(Fig. 3). For simplicity, we let $f(t) \equiv h(a(t - \sigma))$, hence the function $f(t)$ is τ-periodic.

In order to calculate the time-dependent solution of C, we integrate eqn (1) (see the Appendix) to find the difference equation

$$c((n + 1)\tau) = e^{-\delta\tau}\left[c(n\tau) + \int_{t'=0}^{\tau} f(t')e^{\delta t'}dt'\right] \quad (2)$$

for $n \in \{1, 2, \ldots\}$ and hence after rearranging determine,

$$c(n\tau) = \frac{e^{-\delta\tau}}{1 - e^{-\delta\tau}}\int_{t'=0}^{\tau} f(t')e^{\delta t'}dt' \quad (3)$$

as n becomes large.

This gives a periodic solution for integer multiples (n) of the oscillation period τ. We perform a similar calculation for the phase during which the pulse is maximal (namely the GnRHR activated): for $t_1 \in [0, \tau]$,

$$c(n\tau + t_1) \approx e^{-\delta t_1}\int_{t'=0}^{t_1} f(t')e^{\delta t'} \, dt'$$
$$+ e^{-\delta t_1}\frac{e^{-\delta\tau}}{1 - e^{-\delta\tau}}\int_{t'=0}^{\tau} f(t')e^{\delta t'} \, dt', \quad (4)$$

for n large (see the Appendix). Thus, after an initial transient, c is periodic. Integrating eqn (1) gives, in a straightforward way, the average

value, $\bar{c}$ of c,

$$\bar{c} = \frac{1}{\delta}\int_{t'=0}^{\tau} f(t') \, dt' \equiv \frac{\bar{f}}{\delta}, \quad (5)$$

where

$$\bar{f} = \frac{1}{\tau}\int_{t'=0}^{\tau} f(t') \, dt'.$$

Thus, the average is given by an intuitive quantity: the mean activation rate of C divided by its rate of decay. This long-term average is really only interesting biologically if the oscillations around the mean, driven by the pulsatile input, are small relative to the mean. We derive an expression for the mean absolute rate of change of concentration of C:

$$\overline{|\dot{c}|} \equiv \frac{1}{\tau}\int_{n\tau}^{(n+1)\tau} |\dot{c}| \, dt = \frac{1}{\tau}\int_{\{t \in [n\tau, (n+1)\tau], \dot{c} > 0\}} \dot{c} \, dt$$
$$- \frac{1}{\tau}\int_{\{t \in [n\tau, (n+1)\tau], \dot{c} < 0\}} \dot{c} \, dt$$
$$= -\frac{2}{\tau}\int_{\{t \in [n\tau, (n+1)\tau], \dot{c} < 0\}} \dot{c} \, dt \quad (6)$$

for n large, since $\int_{n\tau}^{(n+1)\tau} \dot{c} \, dt \approx 0$, because c is almost τ-periodic. Now (1) implies that $\dot{c} \geqslant -\delta c$, so

$$\overline{|\dot{c}|} < \frac{2\delta}{\tau}\int_{n\tau}^{(n+1)\tau} c \, dt = 2\delta\bar{c}. \quad (7)$$

Thus, if δ is small the average magnitude of the rate of change of c is much less than the average value of c and hence the oscillations in c are proportionally small (see Fig. 4). So, if δ is small, then for $\forall t$ large, $c(t) \approx \bar{f}/\delta$.

MECHANISMS OF AMPLITUDE INDEPENDENCE

If the chemical A comes in pulses of amplitude a_0 and duration $\alpha\tau \equiv \tau_{on}$, then assuming there is no production of C in the absence of A (i.e. $h(0) = 0$) and letting $h(a_0) = s$, $\bar{f} = \alpha s \equiv \tau_{on}/\tau s$ (we note that since c effectively integrates a, the translational time delay, σ, has very little impact on the long-term dynamics) and hence

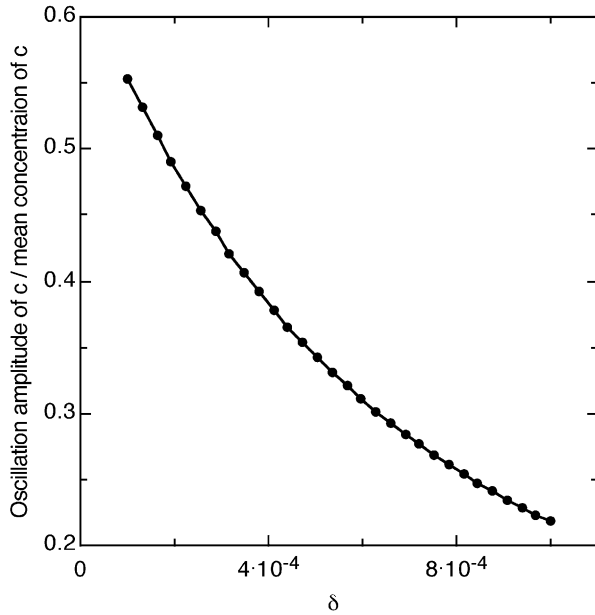$$\bar{c} = \frac{\alpha s}{\delta} \equiv \frac{\tau_{on}s}{\tau\delta}. \quad (8)$$

FIG. 4. The relationship between the mean concentration of egr1 and the oscillation amplitude of egr1, as a function of egr1 decay rate δ. Increasing the decay rate parameter δ leads to a reduction in both the concentration of C and in the amplitude of oscillations. However, oscillations diminish at a larger rate.

If we suppose that the pulses of A have fixed duration τ_{on}, then the system converges to a long-term average concentration in C, with concentration directly proportional to the fre-

quency of the pulses $1/\tau$. The other parameters on which $\bar{c}$ depends are δ, the decay rate of C, and $s = h(a_0) \approx h(\infty)$, assuming a_0 large. This last assumption states, that the amplitude of activation reaches a maximum average value, as a result of the saturating form of the Hill function. This has important computational implications. Namely, that the mean value of c measures the frequency, but not the amplitude (except for very small amplitudes) of the pulses. Thus, varying the instantaneous quantity of GnRH during a pulse should have no effect on the concentration of egr1. Rapid saturation promotes robustness. This module is not, however, a frequency filter in the strictest sense. This is because changes in the pulse duration are indistinguishable from changes in the pulse frequency. This dependency is illustrated in Fig. 5. Increases in pulse duration, keeping the pulse frequency constant, lead to increases in the mean concentration of the component C. Pulse duration and inter-pulse interval are inversely related in their contribution to c.

Model 2: Feed-forward Parallel Network

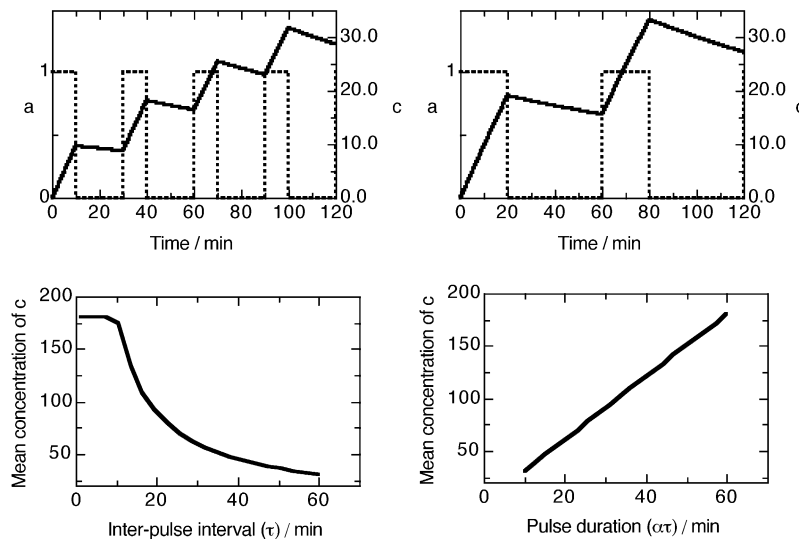We now postulate an alternative network which responds to the frequency of the input

FIG. 5. The impact of varying GnRH (A) pulse duration and pulse frequency on the concentration of the slowly expressed transcription factor egr1 (C). In the top left panel pulse duration is 10 min and pulse period is 30 min. In the top right panel pulse duration is 20 min and pulse period is 60 min. Pulse duration and pulse period are inversely related. This is illustrated over a wide range of pulse frequencies and durations in the lower two panels, in which the long-term average concentration of c ($\bar{c}$) is plotted against pulse duration and inter-pulse interval. This simple circuit cannot separate pulse duration from pulse frequency. $\delta = 0.001$, $\sigma = 10.0$. Concentrations of A and C are denoted by a and c.

without responding to variation in the duration of the pulses. This network goes beyond amplification or integration, to the extraction of specific frequency information. This result is achieved by making use of variation in the time scale of protein activation and gene expression.

Suppose that A (GnRH) activates the production of an intermediate chemical species B (activated MAPK in the GnRH network) which decays fairly rapidly. Suppose B further stimulates production of C (egr1), which decays slowly, but that the presence of A completely blocks this stimulation [Fig. 2(2)]. In other words, GnRH can both stimulate MAPK activation and inhibit the activated MAPK from inducing egr1. The system of equations describing this model are as follows:

$$\dot{b} = h'(a(t)) - pb \equiv f'(t) - pb, \qquad (9)$$

$$\dot{c} = \begin{cases} kb(t-\sigma) - \delta'c, & a = 0, \\ -\delta'c, & a = a_0. \end{cases} \qquad (10)$$

The activation of B only ensues in the presence of A, whereas the production of C only ensues in the presence of activated B. The choice of a piecewise function in our analysis reflects the total inhibition of the expression of C during the activation of A. Integrating eqn (9), analogously to the integration of eqn (1) to derive eqns (3) and (4), yields

$$b(n\tau) = \frac{e^{-pt}}{1 - e^{-pt}} \int_0^\tau f(t) e^{pt} \, dt \quad \text{for } n \text{ large,} \quad (11)$$

$$b(n\tau + t_1) = e^{-pt_1} \left[b(n\tau) + \int_0^{t_1} f(t) e^{pt} \, dt \right] \qquad (12)$$

for $t_1 \in [0, \tau]$.

MECHANISMS OF PULSE-DURATION INDEPENDENCE

Assuming that the activation value has saturated as a Hill-type function, the activation term of the dynamics of b can be replaced by a constant s' when the receptor is stimulated, whereas the activation term is zero when the

input is absent

If $f'(t) = \begin{cases} s', & t \in [n\tau, (n+\alpha)\tau], \\ 0, & t \in [(n+\alpha)\tau, (n+1)\tau], \end{cases}$ then

$$b((n+\alpha)\tau) = \frac{s'}{p} \frac{1 - e^{-p\alpha\tau}}{1 - e^{-p\tau}}, \qquad (13)$$

so for $t \in [(n+\alpha)\tau, (n+1)\tau]$,

$$b(t) = \frac{s'}{p} \frac{1 - e^{-p\alpha\tau}}{1 - e^{-p\tau}} e^{-p(t-(n+\alpha)\tau)}. \qquad (14)$$

Integrating eqn (10), we obtain

$$\bar{c} = \frac{k}{\delta'} \frac{1}{\tau} \int_{\alpha\tau}^{\tau} b(t-\sigma) \, dt. \qquad (15)$$

We are interested in the effects of translational delays on the mean concentration of c. We need to consider two regimes corresponding to short delays (shorter than the pulse duration) and long delays (longer than the pulse duration).

For short delays, $\sigma(\bmod \tau) < \alpha\tau$, this is given by

$$\bar{c} = \frac{k}{\delta'} \frac{1}{\tau} \int_{\alpha\tau - \sigma(\bmod \tau)}^{\tau - \sigma(\bmod \tau)} b \, dt$$

$$= \frac{s'k}{\delta' p^2 \tau} \left[1 + \sigma(\bmod \tau) - e^{-p\sigma(\bmod \tau)} \right.$$

$$\left. \frac{[e^{-p(\tau-\alpha\tau)} + e^{-p\alpha\tau} - 2e^{-p\tau}]}{1 - e^{-p\tau}} \right]. \qquad (16)$$

For long delays, $\sigma(\bmod \tau) > \alpha\tau$, this is given by

$$\bar{c} = \frac{k}{\delta'} \frac{1}{\tau} \left[\int_{\tau + \alpha\tau - \sigma(\bmod \tau)}^{\tau} b \, dt + \int_0^{\tau - \sigma(\bmod \tau)} b \, dt \right]$$

$$= \frac{s'k}{\delta' p^2 \tau} \left[1 + \alpha\tau - e^{-p\sigma(\bmod \tau)} \right.$$

$$\left. \frac{[e^{-p(\tau-\alpha\tau)} + e^{-p\alpha\tau} - 2e^{-p\tau}]}{1 - e^{-p\tau}} \right]. \qquad (17)$$

Thus, the average concentration for any magnitude of delay is given by the shorter of the two

time intervals: $\sigma(\mathrm{mod}\,\tau)$ and $\alpha\tau$:

$$\bar{c} = \frac{s'k}{\delta'p^2\tau}\left[1 + \min[\sigma(\mathrm{mod}\,\tau), \alpha\tau]\right.$$
$$\left. - \mathrm{e}^{-p\sigma(\mathrm{mod}\,\tau)}\frac{[\mathrm{e}^{-p(\tau-\alpha\tau)} + \mathrm{e}^{-p\alpha\tau} - 2\mathrm{e}^{-p\tau}]}{1 - \mathrm{e}^{-p\tau}}\right]. \quad (18)$$

Now if we assume that $\mathrm{e}^{p\tau} \gg \mathrm{e}^{p\alpha\tau} \gg 1$ (corresponding to $\alpha < 1$, $p\tau > 1$, i.e. activated MAPK decays on a shorter time-scale than the period of GnRH oscillations), then

$$\bar{c} \approx \frac{ks'}{\delta'p^2}\frac{1}{\tau}[1 + \min(\sigma(\mathrm{mod}\,\tau), \alpha\tau)]. \quad (19)$$

Thus, if the decay of B is sufficiently fast and the pulses of A sufficiently short, $\bar{c}$ will be directly proportional to the frequency of the pulses. It will depend on the decay rates of B and C, the rate of stimulation of C by B, the strength of activation of B by A, and the minimum of the delay and the duration of the pulses. Since δ' is small, at large times $c \approx \bar{c}$, so c reaches an approximately average concentration at a level proportional to the frequency of the pulses in A. For short delays, the pulse duration is no longer a parameter in the long-term average, and hence the concentration of C is a direct measure of the pulse frequency alone.

<center>AVERAGE RESPONSE PROFILE OF EGR1</center>

This pulse-duration independence is illustrated in Fig. 6. Each of the three right-most panels (right column) differ with respect to the duration of the translational delay term σ. For shorter delays, the range of durations over which the concentrations of C remain unchanged are large. For longer delays, the duration-independent plateau becomes shorter.

Whereas the concentration of C is largely independent from pulse duration, it remains critically dependent upon pulse frequency. In Fig. 6, the three left-most panels (left column) of figures are simulated results for increasing magnitudes of delay. For short delays, there is an increase in the concentration of egr1 with increasing pulse frequency. For long delays, there is a decrease in the concentration of egr1 with increasing pulse frequency. We therefore observe a filtering of pulse frequency, with a peak response at an intermediate frequency, in which this optimum increases with increasing σ.

As we have seen, integration of eqns (9) and (10) yields

$$\bar{c} = \frac{s'k}{\delta'p^2\tau}\left[1 + \min[\sigma(\mathrm{mod}\,\tau), \alpha\tau]\right.$$
$$\left. - \mathrm{e}^{-p\sigma(\mathrm{mod}\,\tau)}\frac{[\mathrm{e}^{-p(\tau-\alpha\tau)} + \mathrm{e}^{-p\alpha\tau} - 2\mathrm{e}^{-p\tau}]}{1 - \mathrm{e}^{-p\tau}}\right]. \quad (20)$$

This is largest when $\sigma = \alpha\tau$ and produces an optimal intermediate value of τ.

Model 3: Recurrent Parallel Network

We now consider a model in which two different time-scales of parallel activation are used to decode frequency. As with model 2, the idea is that the rapid rate of activation and deactivation produced by phosphorylation and dephosphorylation, when in conjunction with the slow rate of activation and deactivation produced by gene expression and protein decay, will produce alternative outputs as a function of variation in input pulse frequency. We consider three components, GnRH denoted by A (concentration denoted by a), activated MAPK phosphatase (MKP) denoted by D (concentration denoted by d) and egr1 denoted by C (concentration denoted by c). A upregulates D (fast species, phosphorylation reaction) and also upregulates C (slow species, gene expression). In addition, D inhibits the upregulation of C by A (through the inactivation of activated MAPK) [Fig. 2(3)]. The dynamics can be described by the following equations:

$$\dot{d} = f(t) - md, \quad (21)$$

$$\dot{c} = \frac{f'(t)}{1 + \mu d} - \delta c, \quad (22)$$

where

$$f(t) = \begin{cases} s, & t \in [n\tau, (n+\alpha)\tau], \\ 0, & t \in [(n+\alpha)\tau, (n+1)\tau], \end{cases} \quad (23)$$

$$f'(t) = \begin{cases} s', & t \in [n\tau + \sigma, (n+\alpha)\tau + \sigma], \\ 0, & t \in [(n+\alpha)\tau + \sigma, (n+1)\tau + \sigma] \end{cases} \quad (24)$$
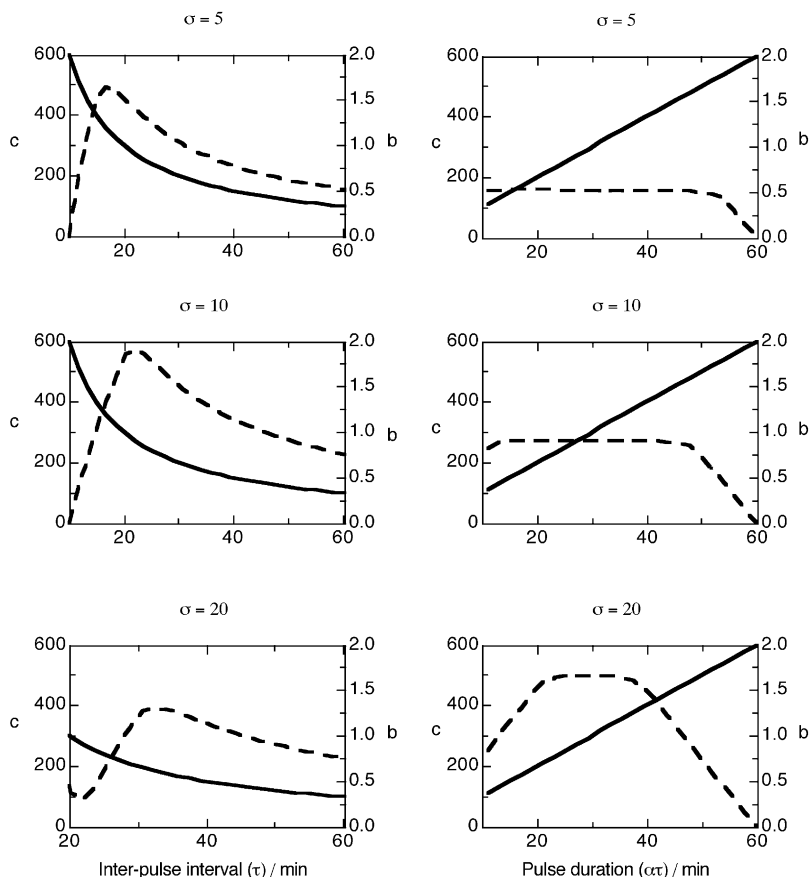
FIG. 6. Frequency detection through parallel activation. The left column panels are the results of simulations for increasing inter-pulse intervals, and the right column for increasing pulse durations. The three rows describe three different magnitudes of translational delay ($\sigma = 5, 10, 20$). A parallel feed-forward network with simultaneous activation and inhibition is able to produce a pulse-duration independent response over a wide range of values. In this range, increasing the pulse duration of GnRH while keeping frequency constant, does not modify the concentration of egr1 (C). For a fixed pulse duration, increasing the inter-pulse interval (reducing the frequency), leads to variation in egr1. Both pulse duration and pulse frequency influence the concentration of activated MAPK. At high- and low-frequencies, egr1 is at low concentrations. At intermediate frequencies — determined by the magnitude of the translational delay — egr1 is at high concentration. $\delta = 0.001$, $m = 0.1$, $k = 1$. Concentrations of B and C are denoted by b and c. Dashed lines are the concentrations of C and solid lines B.

for $n = 1, 2, \ldots.$ As in model 2, we can integrate eqn (21) obtaining

$$d(n\tau + t_1) \approx \begin{cases} \dfrac{s}{m}\left[1 - e^{-mt_1}\left(\dfrac{1 - e^{-m\tau(1-\alpha)}}{1 - e^{-m\tau}}\right)\right], \\ \qquad t_1 \in [0, \alpha\tau], \\[2mm] \dfrac{s}{m} e^{-mt_1}\left(\dfrac{e^{m\tau\alpha} - 1}{1 - e^{-m\tau}}\right), \\ \qquad t_1 \in [\alpha\tau, \tau], \end{cases} \tag{25}$$

for large n.

Now, integrating eqn (18), at large time, we obtain

$$\bar{c} = \frac{1}{\delta\tau}\int_0^\tau \frac{f'}{1 + \mu d}\,dt' = \frac{s'}{\delta\tau}\int_\sigma^{\sigma+\alpha\tau} \frac{1}{1 + \mu d}\,dt'. \tag{26}$$

We now assume that $\sigma > \alpha\tau$ and $\tau > \alpha\tau + \sigma$ (i.e. the duration of a pulse of A is small compared to the translation time of C which is in turn small compared to the inter-pulse interval—the latter condition is not actually necessary, but it makes the analysis easier). In this case, when f' is non-zero, $d(n\tau + t_1) = (s/m)\gamma e^{-m(t_1 - \alpha\tau)}$, where

$\gamma \equiv (1 - e^{-m\tau\alpha}/1 - e^{-m\tau})$. Thus,

$$\bar{c} = \frac{s'}{\delta\tau} \int_{\sigma}^{\alpha\tau+\sigma} \frac{1}{1 + (\mu s\gamma/m)e^{-m(t'-\alpha\tau)}} \, dt' \quad (27)$$

$$= \frac{s'}{\delta\tau} \int_{\sigma-\alpha\tau}^{\sigma} \frac{1}{1 + (\mu s\gamma/m)e^{-mt_1}} \, dt_1 \quad (28)$$

$$= \frac{s'}{m\delta\tau} \ln\left[1 + \frac{e^{m\sigma} - e^{m(\sigma-\alpha\tau)}}{e^{m(\sigma-\alpha\tau)} + (\mu s\gamma/m)}\right]. \quad (29)$$

Now suppose $m\alpha\tau \ll 1$ (i.e. the pulse duration is much shorter than the half-life of B), then $e^{m\sigma} - e^{m(\sigma-\alpha\tau)} \approx m\alpha\tau e^{m\sigma}$, $e^{m(\sigma-\alpha\tau)} \approx e^{m\sigma}$ and $\gamma \approx (m\alpha\tau)/(1 - e^{-m\tau})$, so

$$\bar{c} \approx \frac{s'}{m\delta\tau} \ln\left[1 + \frac{e^{m\sigma}m\alpha\tau}{e^{m\sigma} + \mu s\alpha\tau/(1 - e^{-m\tau})}\right] \quad (30)$$

$$\approx \frac{s'\alpha}{\delta} \frac{1 - e^{-m\tau}}{1 - e^{-m\tau} + \mu s\alpha\tau e^{-m\sigma}}. \quad (31)$$

Let us now assume that the inhibition exerted by B is strong, so that

$$\mu s\alpha\tau e^{-m\sigma} \gg 1 - e^{-m\tau}. \quad (32)$$

(This will be true for all τ if $\mu \gg me^{m\sigma}/(s\alpha)$.) In this case,

$$\bar{c} \approx \frac{s'e^{m\sigma}}{s\mu\delta\tau}(1 - e^{-m\tau}). \quad (33)$$

Thus, for short pulses ($m\alpha\tau \ll 1$) and strong inhibition ($\mu \gg me^{m\sigma}/s\alpha$), $\bar{c}$ is a monotonic decreasing function of τ, with $\bar{c} \approx (s'me^{m\sigma}/s\delta\mu)$ for $\tau = 0$ and $\bar{c} \to 0$, as $\tau \to \infty$. We have assumed so far that $\alpha\tau < \sigma(\text{mod } \tau) < \tau - \alpha\tau$. If instead we assume $\sigma(\text{mod } \tau) < \alpha\tau$ — that the translational delay is shorter than the pulse duration, then

$$\bar{c} = \frac{s'(1 - e^{-m\tau})}{s\mu\delta\tau} \frac{\sigma(\text{mod } \tau)}{\alpha\tau}. \quad (34)$$

Alternatively if the delays are longer than the pulse duration, $\sigma(\text{mod } \tau) > \tau - \alpha\tau$, then

$$\bar{c} = \frac{s'(1 - e^{-m\tau})}{s\mu\delta\tau}e^{m\tau}\frac{\tau - \sigma(\text{mod } \tau)}{\alpha\tau}. \quad (35)$$

So the maximum response occurs for $\tau = \sigma/(n - \alpha)$.

AVERAGE RESPONSE PROFILE OF EGR1

Once again the concentration of C is largely independent from pulse duration. Moreover, in comparison with the parallel network in the previous section, the range of pulse durations over which it remains insensitive is greater for larger delay values. Also worth noting is the rapid drop off in concentration of C outside of this range, giving rise to a switch-like response property. For small and large pulse durations, the concentration of C is effectively zero, whereas at intermediate durations, the concentration is constant.

The egr1 response, as in model 2, is critically dependent on pulse frequency. In Fig. 7, the left column of figures are simulated results for increasing magnitudes of delay. For short delays, there is an increase in the concentration of egr1 with increasing pulse frequency. For long delays, there is a decrease in the concentration of egr1 with increasing pulse frequency. There is filtering of pulse frequency, with a peak response at an intermediate frequency, where this optimum increases with increasing σ. In contrast to model 2, below the optimum pulse frequency, the response drops very rapidly to zero. The response of egr1 is therefore to respond minimally to all pulse frequencies below a threshold value, and then respond with diminishing concentrations to frequencies higher than the peak value ($\tau = \sigma/(n - \alpha)$).

The Responses of Modular Components

We have presented the analysis of three simple models corresponding to putative modules derived from the GnRH signal transduction network. We characterized the response of the modules to pulsatile inputs, determining those features of the pulsatile signal each module was able to efficiently extract. The modules were classified as feed forward when activation propagated from one component to the next without feedback or recurrence. Linear networks had a connectivity of one to one, whereas parallel networks have a connectivity of one to many. Recurrent networks include feedback from distal members of a pathway. The addition of parallel activation or recurrences increase the discrimination ability of the modules. Whereas
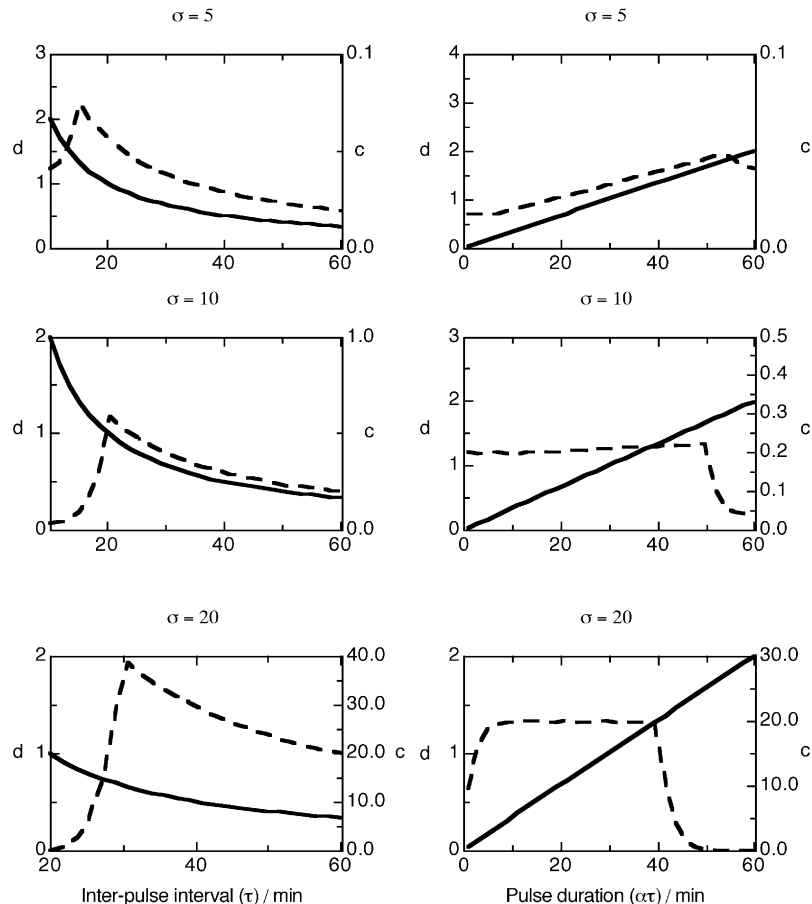
FIG. 7. Peak frequency detection through recurrent, parallel activation. The left column are the results of simulations for increasing inter-pulse intervals, and the right column for increasing pulse durations. The three rows describe three different magnitudes of translational delay. This network renders egr1 (C) insensitive to variation in pulse duration over a wide range of pulse durations. MKP (D) increases with increasing pulse duration. As with module 2, this component is able to respond to increasing pulse frequencies through variation in the concentration of egr1 (C). However, the response of this component is more switch like. High frequencies produce almost no response above threshold. For decreasing frequencies below threshold, the concentration of egr1 drops slowly. Both pulse duration and pulse frequency influence the concentration of activated MAPK, $\delta = 0.001$, $m = 0.1$, $k = 1$. Concentrations of C and D are denoted by c and d. Dashed lines are the concentrations of C and solid lines D.

each of these modules is not independent within a living cell, we have separated them in order that we can better understand their individual response characteristics. An important step towards building a complete network model should include understanding the behavior of its constituent parts.

FEED-FORWARD SERIAL NETWORK

A simple feed-forward design with variable decay rates [module 1, Fig. 1(A)], can act as a signal integrator, or amplifier. Such a network cannot distinguish between constant stimulation and high-frequency stimulation. It functions on the basis of the rapid decay of one chemical species, and the slower decay of another. Slow decay rates permit the accumulation of a component across inter-pulse intervals, serving in effect as a memory molecule. In the GnRH network, it is observed that upon stimulation of the GnRH receptor by its agonist, MAPK is phosphorylated, and that this leads to the production of egr1. Module 1 shows that this design, which could allow for the accumulation of α subunits with increasing frequency, is strictly speaking responding to pulse duration. Thus, a constant signal would prove maximally

effective at eliciting its production. This is at odds with experimental data which suggest a requirement for periodic inputs.

FEED-FORWARD PARALLEL NETWORK

A feed-forward design with parallel activation and inhibition [Module 2, Fig. 1(B)] gives rise to a true frequency decoder. This capability arises out of the fact that the activation of component C is always independent of the activation of A. Thus, C integrates the activity of the decaying component B. The total volume of B detected by C is a function of the inter-pulse interval alone, and hence the frequency of the pulses.

The concurrent rapid activation of MAPK by GnRH and inhibition of egr1, combined with the activation of egr1 through a parallel MAPK pathway, leads to the frequency-dependent production of egr1. This mechanism works by only allowing accumulation of egr1 during the inter-pulse interval, corresponding to the decay phase of MAPK. Thus, egr1 is produced by integrating the activity of the decaying MAPK. This module leads to an increase in egr1 with increasing pulse frequencies up until a threshold frequency, whereupon, egr1 concentration declines monotonically at a slow rate. Increasing the delay resulting from translation of egr1, moves the threshold frequency to lower values.

RECURRENT PARALLEL NETWORK

A recurrent design with parallel activation [module 3, Fig. 1(C)] gives rise to a frequency detector. As with module 1, the network responds to changing frequency by changing the steady-state value of C. As with module 2, the steady-state frequency of C depends non-monotonically on the pulse frequency. At low- and high-frequencies, the steady-state concentration of C is low, whereas at intermediate frequencies, the value of C increases. The module not only responds to frequency information, but it is also tuned to respond maximally to a restricted frequency range. At sufficiently high frequencies, the concentration of egr1 rapidly drops to zero, At low frequencies, the concentration of egr1 falls slowly. The value of D decreases for decreasing pulse frequency monotonically.

GnRH causes a concurrent slow production of egr1 and the rapid activation of MKP. The different time-scales of activation ensure that at high-pulse frequencies, active MKP accumulates and exerts a strong inhibition on the production of egr1. This means that the concentration of egr1 decreases as a function of high-pulse frequencies. At intermediate pulse frequencies, active MKP is unable to accumulate and exerts very little inhibitory effect on the slow accumulation and decay of egr1. At very low pulse frequencies, the slow accumulation of egr1 ensures that it remains at low levels while active MKP can accumulate. Thus, egr1 is maximal at parameter-determined intermediate pulse frequencies. The precise range of values over which egr1 accumulates depends on the delay associated with the translation of egr1.

Signal Transduction, Computation, and Modular Design

Signal transduction describes those reactions through which external stimuli arriving at a cell surface, lead through a series of chemical transformations, to a unique and adaptive cellular response. The stimuli and responses are highly varied, whereas the basic transformations are common to a large number of reactions. The way in which cells increase their range of response, is to use components of signal transduction pathways in combinations, and thereby increase the effective number of pathways. An important consequence of this solution, is that different components, or stages of a network, will appear to have represented different properties of the external stimulus. This is a very general feature of pattern recognition. The visual system processes information in a hierarchical fashion, first extracting contrast information from the optical stimulus (Marr, 1976), combining the contrast information from several cells in order to discern edges (Marr & Hildreth, 1980), and then assembling edges into objects (Marr & Poggio, 1979). Reading from more distal cells in the visual pathway, reveals information of decreasing generality and greater specificity about the stimulus. The same is true of cellular signal transduction, in which only towards the end of a pathway, does there emerge

reliable information about the identity of the stimulus.

The comparison with visual perception, makes clear the interpretation of cellular signal transduction as an information processing task. Following Marr (1982), information processing tasks can be broken down into the computational, algorithmic and implementation levels. Considering the GnRH system, the computational problem is how to turn varying frequencies of ligand binding into different patterns of gene activation. The algorithmic level describes the mechanisms available within the cell for achieving this computation. The implementation level refers to the precise chemical constituents of the GnRH pathways. In this paper, we have considered some of the computational and algorithmic problems of GnRH signal coding. We observed that the earliest stages in the pathways tended to behave much like an integration circuit. Within a circuit, electric charge stores up in a capacitor when voltage is applied to an input. As more charge is stored current flow decreases, whereas the voltage across the capacitor accumulates (integrates). In the simplest feed-forward GnRH circuit, the rapid activation of A leads to a gradual increase in C, which decays away slowly, thereby integrating the activity of A. While the implementation level of circuits and cells is very different, computational tasks and algorithms can be very similar (McAdams & Arkin, 1998, 2000). Cells do not have resistors and capacitors, but they can modify activation-rate constants and decay rates (Judd *et al.*, 2000).

The construction of cellular circuits through the combination of simple elements has been nicely illustrated by Huang & Ferrell (1996) in their work on the mitogen activated protein kinases (MAPKs). A linear, feed-forward arrangement of MAPKs can produce kinetic behavior comparable to that of a highly cooperative enzyme. The modelling of the fission yeast cycle by Sveiczer *et al.* (2000) shows how the addition of recurrence or feedback elements leads to increasing control over the cell cycle. The importance of combining these circuits in a modular fashion has been illustrated by von Dassow *et al.* (2000) for the segment polarity network of Drosophila. Modularity effectively buffers members of a chemical pathway by creating partially self-contained input–output circuits. These studies all serve to highlight the hierarchical and modular architecture of cellular networks. The GnRH system provides a fascinating experimental system in which these issues of computation, hierarchy, and modularity can be explored. Here we have described a few simple modules with response properties that measure the frequency of an incoming stimulus, independent from the amplitude and duration of the pulses. The fundamental mechanism by which this is achieved, is to harness natural variation in protein activation and gene expression rates. This mechanism might have wide application in cellular signalling networks.

REFERENCES

BLUM, J. J., REED, M. C., JANOVICK, J. A. & CONN, P. M. (2000). A mathematical model quantifying GnRH-induced LH secretion from gonadotropes. *Am. J. Physiol. Endocrinol. Metab.* **278,** E263–272.

CHENG, K. W. & LEUNG, P. C. (2000). The expression, regulation and signal transduction pathways of the mammalian gonadotropin-releasing hormone receptor. *Can. J. Physiol. Pharmacol.* **78,** 1029–1052.

CROWLEY, W. F., FILICORI, M., SPRATT, D. I. & SANTORO, N. F. (1985). The physiology of gonadotropin-releasing hormone (GnRH) secretion in men and women. *Rec. Prog. Horm. Res.* **41,** 473–526.

DALKIN, A. C., HAISENLEDER, D. J., ORTOLANO, G. A., ELLIS, T. R. & MARSHALL, J. C. (1989). The frequency of gonadotropin-releasing-hormone stimulation differentially regulates gonadotropin subunit messenger ribonucleic acid expression. *Endocrinology* **125,** 917–924.

GOLDBETER, A., DECROLY, O., LI, Y., MARTIEL, J. L. & MORAN, F. (1988). Finding complex oscillatory phenomena in biochemical systems. An empirical approach. *Biophys. Chem.* **29,** 211–217.

GOLDBETER, A., LI, Y. & DUPONT, G. (1990). Oscillatory dynamics in intercellular communication. *Biomed. Biochim. Acta.* **49,** 935–940.

HAISENLEDER, D. J., DALKIN, A. C., ORTOLANO, G. A., MARSHALL, J. C. & SHUPNIK, M. A. (1991). A pulsatile gonadotropin-releasing hormone stimulus is required to increase transcription of the gonadotropin subunit genes:

evidence for differential regulation of transcription by pulse frequency in vivo. *Endocrinology* **128,** 509–517.

HUANG, C. Y. & FERRELL JR. J. E. (1996). Ultrasensitivity in the mitogen-activated protein kinase cascade. *Proc. Natl Acad. Sci. U.S.A.* **93,** 10078–10083.

JUDD, E. M., LAUB, M. T. & MCADAMS, H. H. (2000). Toggles and oscillators: new genetic circuit designs. *Bioessays* **22,** 507–509.

KAISER, U. B., JAKUBOWIAK, A., STEINBERGER, A. & CHIN, W. W. (1997). Differential effects of gonadotropin-releasing hormone (GnRH) pulse frequency on gonadotropin subunit and GnRH receptor messenger ribonucleic acid levels in vitro. *Endocrinology* **138,** 1224–1231.

KAISER, U. B., SABBAGH, E., CHEN, M. T., CHIN, W. W. & Saunders, B. D. (1998). Sp1 binds to the rat luteinizing hormone beta (LHbeta) gene promoter and mediates gonadotropin-releasing hormone-stimulated expression of the LHbeta subunit gene. *J. Biol. Chem.* **273,** 12943–12951.

LI, Y. & GOLDBETER, A. (1989). Frequency specificity in intercellular communication. Influence of patterns of periodic signaling on target cell responsiveness. *Biophys. J.* **55,** 125–145.

LI, Y. & Goldbeter, A. (1992). Pulsatile signaling in intercellular communication. Periodic stimuli are more efficient than random or chaotic signals in a model based on receptor desensitization. *Biophys. J.* **61,** 161–171.

MARR, D. (1976). Early processing of visual information. *Philos. Trans. R. Soc. Lond. B Biol. Sci.* **275,** 483–519.

MARR, D. (1982). Vision: a Computational Investigation into the Human Representation and Processing of Visual Information. San Francisco: Freeman.

MARR, D. & Hildreth, E. (1980). Theory of edge detection. *Proc. R. Soc. Lond. B Biol. Sci.* **207,** 187–217.

MARR, D. & Poggio, T. (1979). A computational theory of human stereo vision. *Proc. R. Soc. Lond. B Biol. Sci.* **204,** 301–328.

MAURER, R. A., KIM, K. E., SCHODERBEK, W. E., ROBERSON, M. S. & GLENN, D. J. (1999). Regulation of glycoprotein hormone alpha-subunit gene expression. *Recent Prog. Horm. Res.* **54,** 455–484.

MCADAMS, H. H. & ARKIN, A. (1998). Simulation of prokaryotic genetic circuits. *Annu. Rev. Biophys. Biomol. Struct.* **27,** 199–224.

MCADAMS, H. H. & ARKIN, A. (2000). Towards a circuit engineering discipline. *Curr. Biol.* **10,** R318–R320.

NAOR, Z., HARRIS, D. & SHACHAM, S. (1998). Mechanism of GnRH receptor signaling: combinatorial cross-talk of Ca2 + and protein kinase C. *Front Neuroendocrinol.* **19,** 1–19.

NAOR, Z., BENARD, I. & SEGER, I. (2000). Activation of MAPK Cascades by G-protein-coupled receptors: the case of gonadotropin-releasing hormone receptor. *Trends Endocrinol. Metab.* **11,** 91–99.

ROBERSON, M. S., MISRA-PRESS, A., LAURANCE, M. E., STORK, P. J. & MAURER, R. A. (1995). A role for mitogen-activated protein kinase in mediating activation of the glycoprotein hormone alpha-subunit promoter by gonadotropin-releasing hormone. *Mol. Cell. Biol.* **15,** 3531–3539.

SEALFON, S. C., WEINSTEIN, H. & MILLAR, R. P. (1997). Molecular mechanisms of ligand interaction with the gonadotropin-releasing hormone receptor. *Endocr. Rev.* **18,** 180–205

SEGEL, L. A., GOLDBETER, A., DEVREOTES, P. N. & KNOX, B. E. (1986). A mechanism for exact sensory adaptation based on receptor modification. *J. theor. Biol.* **120,** 151–179.

SEVETSON, B. R., SVAREN, J. & MILBRANDT, J. (2000). A novel activation function for NAB proteins in EGR-dependent transcription of the luteinizing hormone beta gene. *J. Biol. Chem* **275,** 9749–9757.

SHUPNIK, M. A. (1990). Effects of gonadotropin-releasing hormone on rat gonadotropin gene transcription in vitro: requirement for pulsatile administration for luteinizing hormone-beta gene stimulation. *Mol. Endocrinol.* **4,** 1444–1450.

SVEICZER, A., CSIKASZ-NAGY, A., GYORFFY, B., TYSON, J. J. & NOVAK, B. (2000). Modeling the fission yeast cell cycle: quantized cycle times in wee1- cdc25Delta mutant cells. *Proc. Natl Acad. Sci. U.S.A.* **97,** 7865–9870.

TREMBLAY, J. J. & DROUIN, J. (1999). Egr-1 is a downstream effector of GnRH and synergizes by direct interaction with Ptx1 and SF-1 to enhance luteinizing hormone beta gene transcription. *Mol. Cell. Biol.* **19,** 2567–2576.

TURGEON, J. L., KIMURA, Y., WARING, D. W. & MELLON, P. L. (1996). Steroid and pulsatile gonadotropin-releasing hormone (GnRH) regulation of luteinizing hormone and GnRH receptor in a novel gonadotrope cell line. *Mol. Endocrinol.* **10,** 439–450.

VON DASSOW, G., MEIR, E., MUNRO, E. M. & ODELL, G. M. (2000). The segment polarity network is a robust developmental module. *Nature* **406,** 188–192.

WECK, J., FALLEST, P. C., PITT, L. K. & Shupnik, M. A. (1998). Differential gonadotropin-releasing hormone stimulation of rat luteinizing hormone subunit gene transcription by calcium influx and mitogen-activated protein kinase-signaling pathways. *Mol. Endocrinol.* **12,** 451–457.

WECK, J., ANDERSON, A. C., JENKINS, S., FALLEST, P. C. & SHUPNIK, M. A. (2000). Divergent and composite gonadotropin-releasing hormone-responsive elements in the rat luteinizing hormone subunit genes. *Mol. Endocrinol.* **14,** 472–485.

WEISS, J., JAMESON, J. L., BURRIN, J. M. & CROWLEY, W. F. (1990). Divergent responses of gonadotropin subunit messenger RNAs to continuous versus pulsatile gonadotropin-releasing hormone in vitro. *Mol. Endocrinol.* **4,** 557–564.

WURMBACH, E., YUEN, T., EBERSOLE, B. J. & SEALFON, S. C. (2001). Gonadotropin releasing hormone receptor-coupled gene gene network organization. *J. Biol. Chem.,* in press.

YOKOI, T., OHMICHI, M., TASAKA, K., KIMURA, A., KANDA, Y., HAYAKAWA, J., TAHARA, M., HISAMOTO, K., KURACHI, H. & MURATA, Y. (2000). Activation of the luteinizing hormone beta promoter by gonadotropin-releasing hormone requires c-Jun NH2-terminal protein kinase. *J. Biol. Chem.* **275,** 21639–21647.

YORDY, J. S. & MUISE-HELMERICKS, R. C. (2000). Signal transduction and the Ets family of transcription factors. *Oncogene* **19,** 6503–6513.

APPENDIX

We show, in this appendix, how eqns (2) and (4) are derived from equation (1)

$$\dot{c} = f(t) - \delta c \Rightarrow (c\dot{e}^{\delta t}) = f(t)e^{\delta t}$$

$$\Rightarrow ce^{\delta t} - c(t_0)e^{\delta t_0} = \int_{t_0}^{t} f(t')e^{\delta t'} dt'$$

$$\Rightarrow c((n+1)\tau)e^{\delta(n+1)\tau}$$

$$= c(n\tau)e^{\delta n\tau} + e^{\delta n\tau}\int_0^{\tau} f(t')e^{\delta t'} dt' \quad (A.1)$$

using the periodicity of f. Dividing by $e^{\delta(n+1)\tau}$ yields (2). Thus, we have a difference equation for $c(n\tau)$. The solution of this is given by eqn (3). Since the difference equation has a constant limiting solution for large n, this shows that the response c tends to a time-periodic solution at large times.

Equation (3) then gives

$$c(n\tau + t_1)e^{n\tau + t_1}$$

$$= c(n\tau)e^{n\tau} + e^{n\tau}\int_0^{t_1} f(t')e^{\delta t'} dt'. \quad (A.2)$$

Dividing by $e^{n\tau + t_1}$ and substituting for $c(n\tau)$ from eqn (3) yields eqn (4).